Check for updates

Zeolites Hot Paper

How to cite: *Angew. Chem. Int. Ed.* **2022,** *61,* e202203903
International Edition: doi.org/10.1002/anie.202203903
German Edition: doi.org/10.1002/ange.202203903

Exploring the Influence of Inter- and Intra-crystal Diversity of Surface Barriers in Zeolites on Mass Transport by Using Super-Resolution Microimaging of Time-Resolved Guest Profiles

Shichao Peng, Yiwei Xie, Linying Wang, Wenjuan Liu, Hua Li, Zhaochao Xu, Mao Ye,* and Zhongmin Liu*

Abstract: The applications of nanoporous crystalline materials are closely related to the mass transfer of guest molecules. However, the fundamental knowledge of mass transfer, and in particular the surface barriers controlled by the permeation of guest molecules through the external surfaces of materials, is still incomplete. The diversity of surface permeability at the single-crystal level, caused by the varying origins of surface transport resistance, hinders the rational materials design and needs better understanding. Herein, we probe the molecular transport in single zeolite crystals with fluorescent 4-(4-diethylaminostyryl-1-methylpyridinium iodide) (DAMPI) using super-resolution structured illumination microscopy (SIM). It showed that both the inter- and intra-crystal diversity of surface barriers could be monitored by detecting the diffusion behaviors on the center and surface planes in single crystals. This adds a new perspective for studying the origins of the surface barriers as well as the molecular transport mechanisms in nanoporous materials.

Nanoporous materials find widespread applications in processes spanning heterogeneous catalysis and adsorption separation due to their unique shape selectivity, in which mass transfer between the host crystals and the surrounding guest molecules plays an essential role.[1] The effective control of these nanoporous-material-based processes requires deep understanding of the underlying molecular transport mechanisms.

[*] S. Peng, Y. Xie, Dr. L. Wang, Dr. H. Li, Prof. Dr. M. Ye, Prof. Dr. Z. Liu
National Engineering Research Center of Lower-Carbon Catalysis Technology, Dalian National Laboratory for Clean Energy, Dalian Institute of Chemical Physics, Chinese Academy of Sciences
Dalian 116023 (P. R. China)
E-mail: lihua@dicp.ac.cn
maoye@dicp.ac.cn
W. Liu, Prof. Dr. Z. Xu
Key Laboratory of Separation Science for Analytical Chemistry, Dalian Institute of Chemical Physics, Chinese Academy of Sciences
Dalian 116023 (P. R. China)
S. Peng, Y. Xie, W. Liu, Prof. Dr. Z. Liu
University of Chinese Academy of Sciences
Beijing 100049 (P. R. China)

In general, there are two mass transfer mechanisms, i.e. intracrystalline diffusion and surface barriers, respectively.[2] The former refers to the molecular diffusion inside the pore network and is related to the topological structure and internal grain boundaries, while the latter originates from the molecular permeation through the external surface, most likely attributed to the imperfect morphologies of crystal surfaces.[3] Recent studies show both mechanisms can possess great impact on the heterogeneous catalytic processes.[4] However, compared with the well-established intracrystalline diffusion, surface barriers are yet to be understood in these processes. Essentially tracing out the interaction between guest molecules and surfaces of host crystals is highly desired to unveil the detailed surface transport mechanism and guide the rational design of full-featured zeolite catalysts.

The quantification of mass transfer can stem from either uptake or release measurement using both macro- and microscopic techniques. Most macroscopic methods, i.e. zero length column (ZLC),[5] frequency response (FR)[6] and intelligence gravimetric analyzer (IGA),[7] however, are generally utilized to obtain the apparent diffusivity. The apparent diffusivity is the representative of the overall diffusion behavior of guest molecules and fails to directly distinguish the surface barriers from intracrystalline diffusion in the transport mechanisms, except for the uptake method recently proposed by Gao et al.[7] On the other hand, Karger and co-workers have developed interference microscopy and infrared microscopy for perceiving the time-dependent guest profiles at single-crystal level.[8] Though the micro-imaging techniques play a unique role in correctly unveiling the surface-barrier-limited process, reasonable distinction of transport mechanisms to illustrate the diversity of surface permeability at single crystal level, which caused the varying origins of surface transport resistance, still remains a non-trivial task.[8e]

Super-resolution fluorescence microscopies have been successfully extended to the heterogeneous catalysis and porous material characterization.[9] Compared with the interference microscope that requires large crystal ($\approx$50 μm) in the measurements, super-resolution techniques show higher imaging resolution and thus can be utilized to detect smaller crystals with size of industrial interest. Moreover, as a consequence of the flexible and adjustable confocal plane, the fluorescence signal of each cross section in the individual crystal can be obtained. It provides the opportunity to record the process of

© 2022 Wiley-VCH GmbH

the guest molecules entering the middle zone of an individual zeolite as well as absorbing at the crystal surface. In this work, we use super-resolution structured illumination microscopy (SIM) to reveal the inter- and intra-crystal diversity in surface mass transfer in single ZSM-5 zeolite crystal by use of fluorescent 4-(4-diethylaminostyryl-1-methylpyridinium iodide) (DAMPI) probes.

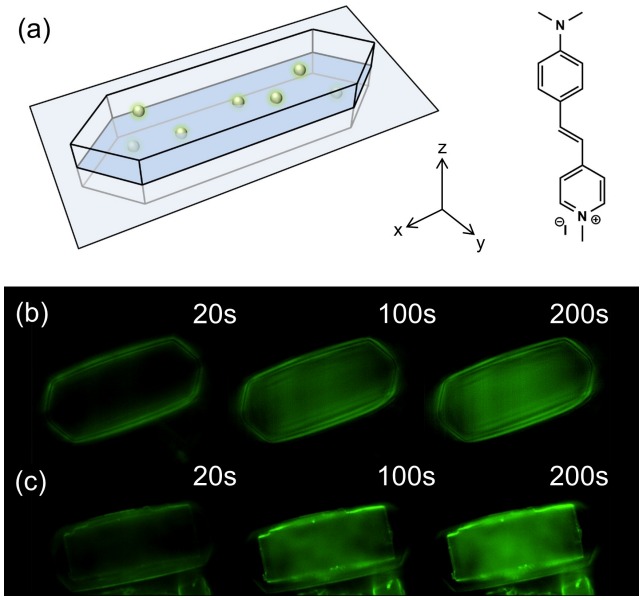

Figure 1. a) Schematic representation of the super-resolution fluorescence microscopy approach and luminescence of DAMPI probes. b, c) Time-resolved SIM images on the middle (b) and top (c) plane of ZSM-5 individual crystal placed in DAMPI solution.

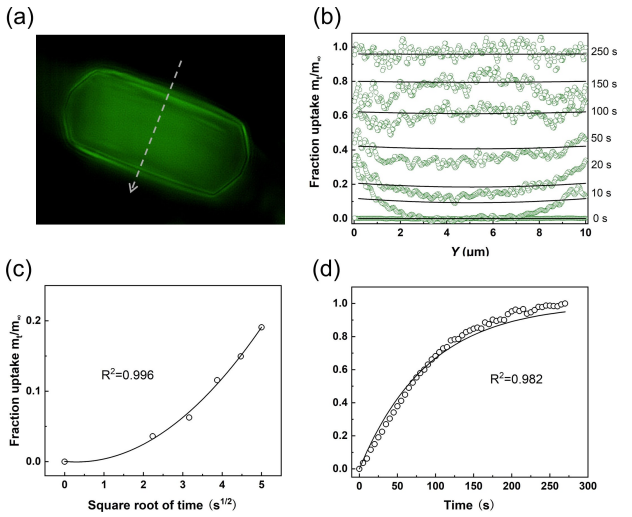

Figure 2. a) SIM images on the middle plane of ZSM-5 with crystal dimensions. b) 1D concentration profiles along *Y* axis. c, d) Initial (c) and overall (d) uptake curves of DAMPI probes in ZSM-5 single crystal. The scatters are the experimental data while solid lines represent fitting results by Eq. (S1) (b), Eq. (1) (c) and Eq. (2) (d). R^2 represents the correlation coefficient.

Figure 1 illustrates the host–guest interaction of fluorescent probes in single ZSM-5 crystal recorded by super-resolution fluorescence microscopy. Here, we prepared a batch of coffin-shaped ZSM-5 crystals with the size of $20\times10\times10\ \mu m^3$ for the SIM tests, in which DAMPI was used as a probe due to its stable excitation at the wavelength of 488 nm.[10] By use of SIM we monitored the evolution of fluorescence signal of the time-dependent guest profiles on different confocal planes (Figure 1a). As shown in Figure 1b, the simultaneous adsorption and diffusion of the DAMPI probe on the central section of the single ZSM-5 crystal can be observed by SIM when focusing on the middle plane of crystal, which directly shows a gradual absorption during the surface transport of guest molecules. If confocal to the top plane, the accumulation of the probe on the crystal surface can be captured. As can be seen in Figure 1c, the fluorescence firstly appears on the outer rim of the crystal, and then gradually fills the entire zeolite, representing the coupling of surface permeation and intracrystalline diffusion in the zeolite crystal. By means of these time-resolved spectrograms, we can further explore the diffusion of guest molecules on the external surface of zeolites.

Figure 2 shows the DAMPI probe concentration evolution of single ZSM-5 crystals. Figure 2a is the fluorescence signals from the central plane of one typical crystal (number 1) recorded by time-resolved SIM. For a specific recognition of its transport mechanisms, the central axis data is selected to analyze the diffusion behavior of the individual zeolite. As shown in Figure 2b, the normalized concentration represents the coupling process of surface permeation and intracrystalline diffusion. Its boundary concentration slowly rises, manifesting the existence of surface barriers, which prevent the guest molecules from permeation through the crystal surface. Besides, the rapid equilibrium between intracrystalline and boundary concentration shows the smooth diffusion inside this crystal, indicating that the transport limitation is dominant by the surface barriers.

To further quantify the surface permeability (α) and intracrystalline diffusion (D) of DAMPI in ZSM-5 crystals, the uptake method was utilized to decouple the cumulative fluorescence signal. Here, a concise quadratic formula proposed for directly quantifying the surface barriers through the initial uptake curves[7] is considered:

$$\frac{m_t}{m_\infty}\Big|^{\sqrt{t}\to 0} \cong \frac{\alpha}{l}\left(\sqrt{t}\right)^2 \tag{1}$$

here m_t/m_∞ and l denote, respectively, the normalized loading at the uptake time t and the equivalent radius of the zeolite crystal. Then, the whole uptake can be further fitted to obtain the intracrystalline diffusivity with dual resistance model (DRM) according to:

© 2022 Wiley-VCH GmbH

$$\frac{m_t}{m_\infty} = 1 - \sum_{n=1}^{\infty} \frac{2L^2 \exp\left(-\frac{\beta_n^2 Dt}{l^2}\right)}{(\beta_n^2 + L^2 + L)\beta_n^2}; \qquad \beta_n \tan\beta_n = L = \frac{\alpha l}{D} \tag{2}$$

In this way, the initial (Figure 2c) and overall (Figure 2d) uptake rates of probe in this crystal can be used to obtain the corresponding surface permeability and intracrystalline diffusivity. Here, five different lookalike crystals were selected out of a batch of ZSM-5 zeolites for diffusion determination. As shown in Table 1, these series of crystals show different surface permeability and similar intracrystalline diffusivity, which implies the diversity of surface barriers with consistent internal diffusion. This demonstrates that even though the crystals are synthesized with same conditions and have consistent internal topology structure, resulting in the same intracrystalline diffusivity, the intercrystal variation in transport properties does exist at single crystal level mainly owing to the distinct surface resistance. The diversity in molecular diffusion may be caused by the inconsistency of the external surface environment of each crystal, which would originate from the complexity of crystal growth mechanism even in the same batches of zeolites.

Table 1: Surface permeability and intracrystalline diffusivity of ZSM-5 crystals.

Crystal number	Surface permeability [$m\,s^{-1}$]	Intracrystalline diffusivity [$m^2\,s^{-1}$]
1	2.32×10^{-8}	9.2×10^{-11}
2	2.76×10^{-8}	9.4×10^{-11}
3	3.06×10^{-8}	9.7×10^{-11}
4	3.64×10^{-8}	8.5×10^{-11}
5	4.25×10^{-8}	8.9×10^{-11}

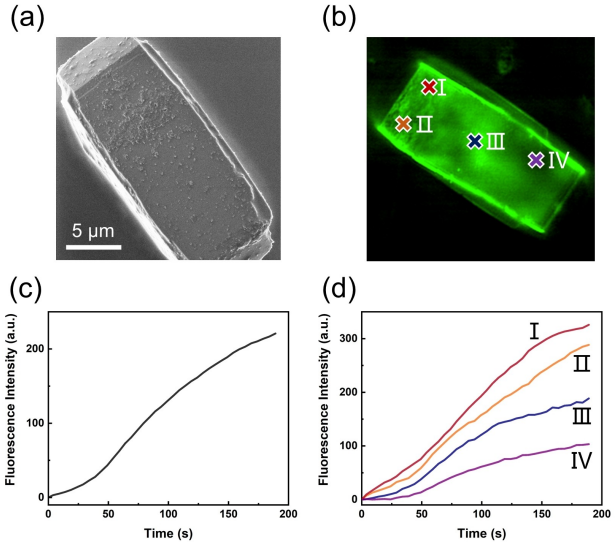

Figure 3. a) HIM images of ZSM-5 crystal. b) SIM images on the top plane of ZSM-5 with crystal dimensions. c, d) The average global (c) and local (d) fluorescent signal evolution of the above crystal surface (b). Numbers in (d) correspond to (b).

The imperfect structure on the crystal surface is considered to be an essential cause of surface barriers.[3b] A clear observation of the ZSM-5 crystal morphology was recorded by helium ion microscopy (HIM) (Figure 3a), showing an obvious layer of amorphous-alike phase which implies the non-ideal construction of ZSM-5 crystal surface. This may be one of the origins of surface barriers. Figure 3b shows the SIM images from the top plane of a typical ZSM-5 crystal selected to determine the mass transport of DAMPI probe on the crystal surface. Based on the evolution of the overall fluorescence intensity shown in Figure 3c, it seems the concentration of DAMPI probe on the top plane of crystal does not reach an instant equilibrium with the surroundings, which instead demonstrates a slow increase. This finding adds a new piece of evidence on the existence of surface barriers. To understand the intra-crystal diversity of surface transport within a single zeolite crystal, we further monitored the fluorescence signal evolution of four random areas ($0.3\,\mu m \times 0.3\,\mu m$) on this ZSM-5 crystal surface. As shown in the Figure 3d, the increase in the average fluorescent signal intensity of these areas vary to a large extent, which indicates that the external permeation of the guest molecules through the individual crystal surface is not uniform and shows an obvious intra-crystal diversity within a single zeolite. This heterogeneity within a single crystal may be related to the rugged surface morphology. Due to the obstruction of surface sediments, the guest molecules would not be able to directly enter the pore, which leads to the circumnavigation on the external surface, resulting in the nonuniformity of the surface permeation.

In conclusion, we for the first time adopt a super-resolution imaging technique to investigate the surface barriers at the single-crystal scale. The adsorption and diffusion of the guest molecules on the external surface and central section of the individual ZSM-5 crystal was tracked by time-resolved structured illumination microscopy in combination with fluorescent DAMPI probes. By directly decoupling and quantifying the surface mass transfer behavior, we further demonstrate the intra- and inter-crystal diversity in surface barriers with batches of zeolites. It provides a new strategy for in-depth understanding of mass transfer at the single-crystal scale, which can be potentially applied to other crystalline materials, such as metal–organic frameworks (MOFs) and covalent-organic frameworks (COFs). This work provides detailed knowledge of surface mass transfer mechanisms, which could enhance the efficiency of nanoporous crystalline materials in heterogeneous catalysis and separation technologies.

Acknowledgements

This work is supported by the National Natural Science Foundation of China (Grant No. 21991093) and Innovation program of science and research from Dalian Institute of Chemical Physics (DICP I201938).

© 2022 Wiley-VCH GmbH

Conflict of Interest

The authors declare no competing financial interests.

Data Availability Statement

The data that support the findings of this study are available from the corresponding author upon reasonable request.

Keywords: Guest Molecules · Mass Transfer · Structured Illumination Microscopy · Surface Barriers · Zeolites

[1] a) G. T. Whiting, N. Nikolopoulos, I. Nikolopoulos, A. D. Chowdhury, B. M. Weckhuysen, *Nat. Chem.* **2019**, *11*, 23–31; b) U. Olsbye, S. Svelle, M. Bjorgen, P. Beato, T. V. Janssens, F. Joensen, S. Bordiga, K. P. Lillerud, *Angew. Chem. Int. Ed.* **2012**, *51*, 5810–5831; *Angew. Chem.* **2012**, *124*, 5910–5933; c) Y. Wu, S. Zeng, D. Yuan, J. Xing, H. Liu, S. Xu, Y. Wei, Y. Xu, Z. Liu, *Angew. Chem. Int. Ed.* **2020**, *59*, 6765–6768; *Angew. Chem.* **2020**, *132*, 6831–6834; d) S. Gao, S. Xu, Y. Wei, Q. Qiao, Z. Xu, X. Wu, M. Zhang, Y. He, S. Xu, Z. Liu, *J. Catal.* **2018**, *367*, 306–314.

[2] a) L. Heinke, Z. Gu, C. Woll, *Nat. Commun.* **2014**, *5*, 4562; b) J. Kärger, D. M. Ruthven, *New J. Chem.* **2016**, *40*, 4027–4048; c) S. Vasenkov, J. Karger, *Microporous Mesoporous Mater.* **2002**, *55*, 139–145; d) A. Feldhoff, J. Caro, H. Jobic, J. Ollivier, C. B. Krause, P. Galvosas, J. Kaerger, *ChemPhysChem* **2009**, *10*, 2429–2433.

[3] a) L. Karwacki, E. Stavitski, M. H. Kox, J. Kornatowski, B. M. Weckhuysen, *Angew. Chem. Int. Ed.* **2007**, *46*, 7228–7231; *Angew. Chem.* **2007**, *119*, 7366–7369; b) L. Karwacki, M. H. Kox, D. A. de Winter, M. R. Drury, J. D. Meeldijk, E. Stavitski, W. Schmidt, M. Mertens, P. Cubillas, N. John, A. Chan, N. Kahn, S. R. Bare, M. Anderson, J. Kornatowski, B. M. Weckhuysen, *Nat. Mater.* **2009**, *8*, 959–965; c) L. Karwacki, H. E. van der Bij, J. Kornatowski, P. Cubillas, M. R. Drury, D. A. de Winter, M. W. Anderson, B. M. Weckhuysen, *Angew. Chem. Int. Ed.* **2010**, *49*, 6790–6794; *Angew. Chem.* **2010**, *122*, 6942–6946.

[4] a) S. Peng, M. Gao, H. Li, M. Yang, M. Ye, Z. Liu, *Angew. Chem. Int. Ed.* **2020**, *59*, 21945–21948; *Angew. Chem.* **2020**, *132*, 22129–22132; b) S. Peng, H. Li, W. Liu, J. Yu, Z. Xu, M. Ye, Z. Liu, *Chem. Eng. J.* **2022**, *430*, 132760; c) S. M. Rao, E. Saraçi, R. Gläser, M.-O. Coppens, *Chem. Eng. J.* **2017**, *329*, 45–55; d) G. Ye, Y. Sun, Z. Guo, K. Zhu, H. Liu, X. Zhou, M.-O. Coppens, *J. Catal.* **2018**, *360*, 152–159; e) Z. Guo, X. Li, S. Hu, G. Ye, X. Zhou, M.-O. Coppens, *Angew. Chem. Int. Ed.* **2020**, *59*, 1548–1551; *Angew. Chem.* **2020**, *132*, 1564–1567; f) S. Hu, J. Liu, G. Ye, X. Zhou, M. O. Coppens, W. Yuan, *Angew. Chem. Int. Ed.* **2021**, *60*, 14394–14398; *Angew. Chem.* **2021**, *133*, 14515–14519.

[5] a) A. R. Teixeira, C.-C. Chang, T. Coogan, R. Kendall, W. Fan, P. J. Dauenhauer, *J. Phys. Chem. C* **2013**, *117*, 25545–25555; b) A. R. Teixeira, X. Qi, W. C. Conner, T. J. Mountziaris, W. Fan, P. J. Dauenhauer, *Chem. Mater.* **2015**, *27*, 4650–4660.

[6] a) O. C. Gobin, S. J. Reitmeier, A. Jentys, J. A. Lercher, *J. Phys. Chem. C* **2009**, *113*, 20435–20444; b) S. J. Reitmeier, O. C. Gobin, A. Jentys, J. A. Lercher, *Angew. Chem. Int. Ed.* **2009**, *48*, 533–538; *Angew. Chem.* **2009**, *121*, 541–546.

[7] M. Gao, H. Li, M. Yang, S. Gao, P. Wu, P. Tian, S. Xu, M. Ye, Z. Liu, *Commun. Chem.* **2019**, *2*, 43.

[8] a) D. Tzoulaki, L. Heinke, W. Schmidt, U. Wilczok, J. Karger, *Angew. Chem. Int. Ed.* **2008**, *47*, 3954–3957; *Angew. Chem.* **2008**, *120*, 4018–4021; b) F. Hibbe, C. Chmelik, L. Heinke, S. Pramanik, J. Li, D. M. Ruthven, D. Tzoulaki, J. Karger, *J. Am. Chem. Soc.* **2011**, *133*, 2804–2807; c) J. Kärger, T. Binder, C. Chmelik, F. Hibbe, H. Krautscheid, R. Krishna, J. Weitkamp, *Nat. Mater.* **2014**, *13*, 333–343; d) J. Kärger, *Microporous Mesoporous Mater.* **2014**, *189*, 126–135; e) J. C. Saint Remi, A. Lauerer, C. Chmelik, I. Vandendael, H. Terryn, G. V. Baron, J. F. Denayer, J. Karger, *Nat. Mater.* **2016**, *15*, 401–406.

[9] a) Z. Ristanović, J. P. Hofmann, G. De Cremer, A. V. Kubarev, M. Rohnke, F. Meirer, J. Hofkens, M. B. Roeffaers, B. M. Weckhuysen, *J. Am. Chem. Soc.* **2015**, *137*, 6559–6568; b) Z. Ristanović, M. M. Kerssens, A. V. Kubarev, F. C. Hendriks, P. Dedecker, J. Hofkens, M. B. Roeffaers, B. M. Weckhuysen, *Angew. Chem. Int. Ed.* **2015**, *54*, 1836–1840; *Angew. Chem.* **2015**, *127*, 1856–1860; c) X. Wu, S. Xu, W. Zhang, J. Huang, J. Li, B. Yu, Y. Wei, Z. Liu, *Angew. Chem. Int. Ed.* **2017**, *56*, 9039–9043; *Angew. Chem.* **2017**, *129*, 9167–9171; d) F. C. Hendriks, F. Meirer, A. V. Kubarev, Z. Ristanovic, M. B. J. Roeffaers, E. T. C. Vogt, P. C. A. Bruijnincx, B. M. Weckhuysen, *J. Am. Chem. Soc.* **2017**, *139*, 13632–13635; e) T. Chen, B. Dong, K. Chen, F. Zhao, X. Cheng, C. Ma, S. Lee, P. Zhang, S. H. Kang, J. W. Ha, W. Xu, N. Fang, *Chem. Rev.* **2017**, *117*, 7510–7537.

[10] F. C. Hendriks, J. E. Schmidt, J. A. Rombouts, K. Lammertsma, P. C. A. Bruijnincx, B. M. Weckhuysen, *Chem. Eur. J.* **2017**, *23*, 6305–6314.

Manuscript received: March 15, 2022
Accepted manuscript online: May 19, 2022
Version of record online: June 8, 2022

© 2022 Wiley-VCH GmbH